

## RESEARCH ARTICLE

### Calculation of viscoelastic bead-rod flow mediated by a homogenized kinetic scale with holonomic constraints

B. Kallemov<sup>a</sup>, G. H. Miller<sup>b\*</sup>, S. Mitran<sup>c</sup>, and D. Trebotich<sup>d</sup>

<sup>a</sup>Nazarbayev University, Astana, Kazakhstan; <sup>b</sup>University of California, Davis, CA, 95616, USA;

<sup>c</sup>University of North Carolina, Chapel Hill, NC, 27599, USA; <sup>d</sup>Lawrence Berkeley National Laboratory, Berkeley, 94720, CA, USA

(Received 00 Month 200x; final version received 00 Month 200x)

We present a new multiscale model for complex fluids based on three scales: microscopic, kinetic, and continuum. We choose the microscopic level as Kramers' bead-rod model for polymers, which we describe as a system of stochastic differential equations with an implicit constraint formulation. The associated Fokker-Planck equation is then derived, and adiabatic elimination removes the fast momentum coordinates. Approached in this way, the kinetic level reduces to a dispersive drift equation. The continuum level is modeled with a finite volume Godunov-projection algorithm. We demonstrate computation of viscoelastic stress divergence using this multiscale approach.

**Keywords:** viscoelasticity, complex fluids, multiscale, microfluidics

## 1 INTRODUCTION

Complex fluids are characterized by microscopic constituents whose internal configuration influences momentum transfer observed at a macroscopic scale, at which the fluid can be considered a continuum. The flow of an incompressible viscoelastic fluid at macroscopic length scales is given by the momentum equation

$$\frac{\partial \mathbf{u}}{\partial t} + \mathbf{u} \cdot \nabla \mathbf{u} + \frac{1}{\rho} \nabla P = \nu \Delta \mathbf{u} + \frac{1}{\rho} \nabla \cdot \boldsymbol{\tau}, \quad (1)$$

together with the conservation of mass for an incompressible fluid

$$\nabla \cdot \mathbf{u} = 0. \quad (2)$$

In this formulation,  $\rho \nu \Delta \mathbf{u}$  is the divergence of a viscous (Newtonian) stress tensor. This term alone accounts for the rheology of many simple fluids. But, when polymers are suspended in the fluid they contribute an extra stress  $\boldsymbol{\tau}$  to the system. To simulate a system like (1),(2) a closure is needed to relate the viscoelastic stress to the fluid velocity,  $\boldsymbol{\tau}(\mathbf{x}, t, \mathbf{u})$ . A variety of macroscopic constitutive closure relations have been proposed to approximate at the continuum level the dynamics associated with the molecular scale, among which we consider the class of relations in partial differential equation (PDE) form. For instance, the Oldroyd-B [24] PDE describes a dilute (non-interacting) suspension of infinitely-extensible springs connected to point masses which interact with the fluid by Stokes drag. Despite the great simplicity of this model,

---

\*Corresponding author. Email: grgmiller@ucdavis.edu

it adequately represents the constitutive behavior of a class of fluids (Boger fluids) under restricted flow regimes. The approximation of a polymer by a spring is motivated by the statistical mechanics result that a freely-jointed polymer obeys length distribution statistics that are approximately Gaussian: a long polymer is approximately a spring, and the motive force is entropic. In flows with large shears, the Oldroyd-B model overestimates the extension of the polymers, which is finite for a physical polymer but unbounded in the entropic spring approximation. A compensating force can be added to the constitutive model to prevent overextension, resulting in the FENE-P model [3]. Models of greater complexity have been proposed to correct limitations of these simple constitutive closures, but there are limits to the ability of a macroscopic constitutive model to approximate the dynamics associated with the large number of degrees of freedom contained in even simple models of a linear polymer [1, 2].

This motivates a multiscale approach, where the extra stress  $\boldsymbol{\tau}$  is obtained in some manner from a molecular scale model, and provided as a source term to a continuum-level numerical method for (1),(2). A pioneering approach along these lines is the CONNFFESSIT method [18] which represents dumbbell polymers as a system of stochastic differential equations (SDE). A drawback of the approach is the enormous number of SDEs that must be solved for even a simple system. Mitran [22] introduced two ideas that improve the performance of such multiscale models: the association of a kinetic scale between the continuum and molecular and levels, and the use of time-parallelism to make a very fast implementation using graphical processing units.

In prior work [11, 12] we developed new high-order numerical methods for the simulation of a Kramers bead-rod freely-jointed polymer, that is, a set of  $N$  “beads,” point masses subject to Stokes drag and Brownian motion, connected by  $N - 1$  “rods,” massless objects meant to keep the beads at constant relative separation. “Freely-jointed” means the rods can interpenetrate. A single polymer is given by the following system of constrained SDEs:

$$\frac{\partial \mathbf{q}_i}{\partial t} = \mathbf{v}_i \tag{3a}$$

$$\frac{\partial \mathbf{v}_i}{\partial t} = \gamma(\mathbf{u}(\mathbf{q}_i, t) - \mathbf{v}_i) + \sigma \boldsymbol{\xi}_i \tag{3b}$$

$$\|\mathbf{q}_{i+1} - \mathbf{q}_i\| = a. \tag{3c}$$

Here,  $i \in [1, N]$  labels beads.  $\mathbf{q}_i, \mathbf{v}_i$  are the coordinate and velocity of bead  $i$ , respectively, in the  $D$ -dimensional (2 or 3) space being simulated.  $\boldsymbol{\xi}_i$  is a vector of uncorrelated white noise associated with bead  $i$ , and  $a$  is the inter-bead spacing, commonly associated with the polymer Kuhn length. The parameter  $\sigma$  is given by

$$\sigma = \sqrt{\frac{2\gamma k_B T}{m}} \tag{4}$$

where  $m$  is the mass of a bead. The drag term  $\gamma(\mathbf{u} - \mathbf{v})$  provides a coupling of the macroscopic flow to the microscale simulation. By itself, this model can calculate a number of classical results including the mean end-to-end distance in relaxed flow, and velocity correlations along the chain. We have also developed numerical schemes for coupling individual polymers with microfluidic flows [10, 13, 14]. This work, like CONNFFESSIT, couples directly the continuum and microscale dynamics.

Here, we present progress toward a continuum–kinetic–molecular multiscale model for dilute freely-jointed polymers in a Newtonian solvent. Kramers’ freely-jointed model has finite extensibility and possesses a spectrum of relaxation times which differ by as much as  $N^2$  for an  $N$ -bead polymer. Thus, while still highly idealized, Kramers’ model nonetheless possesses significant complexity and many more degrees of freedom than any practical macroscopic closure approximation. The emphasis here will be on the kinetic (mesoscale) layer of the multiscale scheme. We present new algorithms for the calculation and time propagation of this description,

and show preliminary results.

## 2 A MULTISCALE FRAMEWORK

To motivate our choice of kinetic approximation, we briefly describe here the framework for our continuum–kinetic–molecular approach to the solution of (1),(2) with extra stress  $\boldsymbol{\tau}$  derived from a dilute suspension of Kramers’ “polymers” modeled by (3).

Since the number of polymers contained in any macroscopic volume can be large, say  $\mathcal{O}(10^{23})$ , it is impossible to represent the state of a particular volume element by specifying the field variables  $\mathbf{u}, P$ , and all relevant microscopic variables  $\{\mathbf{q}, \mathbf{v}\}$ . Instead, we will use the representation  $\mathbf{u}, P, \psi$  where  $\psi(\mathbf{q}, t)$  is the probability density function (PDF): the probability of the existence of a polymer having configuration  $\mathbf{q}$  at time  $t$ .

Formally,  $\psi$  depends on all coordinate and velocity variables,  $\mathcal{O}(2ND \times 10^{23})$ . We will consider the dilute limit where individual polymers do not interact. We will assume a mean field approximation: the influence of one polymer on another is mediated by the continuum fluid field  $\mathbf{u}$ . The velocity of individual “beads” is essentially thermally distributed about the mean fluid velocity  $\mathbf{u}$ . The time scale on which this distribution forms is  $1/\gamma$ , which is much smaller than a typical continuum scale time step. Therefore, on continuum time scales there is a separation of variables. With velocity variables characterized by a thermal distribution, only the spatial part  $\psi(\mathbf{q}, t)$  is needed to characterize the polymer probability density.

Let  $\psi(\bar{\mathbf{q}} | \mathbf{x}, t)$  be the PDF at time  $t$  at point in space  $\mathbf{x}$ , where  $\bar{\mathbf{q}}$  is the vector of bead coordinates relative to the center of mass  $\mathbf{x}$ . Subject to the assumptions outlined above, sampling  $\psi(\bar{\mathbf{q}} | \mathbf{x}, t)$  at time  $t$  allows one to generate a representative instantiation of a polymer  $\mathbf{q}(t)$ . We assume a microscopic time-scale sufficiently large for thermal equilibration to have occurred such that a temperature for the polymer chains can be defined. Under this assumption the velocity  $\mathbf{v}(t)$  is generated by sampling a Boltzmann distribution. Then, using a high-order numerical SDE method [11], a polymer configuration may be advanced in time to give  $\mathbf{q}(t + \Delta t), \mathbf{v}(t + \Delta t)$ . Repeating this process many times, one determines a set of polymer configurations at  $t + \Delta t$ , which must be consistent with a new PDF  $\psi(\bar{\mathbf{q}} | \mathbf{x} + \mathbf{u}\Delta t, t + \Delta t)$ :

$$\psi(\bar{\mathbf{q}} | \mathbf{x}, t) \rightarrow \left. \begin{array}{l} \text{sample} \\ \left\{ \begin{array}{l} \mathbf{q}(t), \mathbf{v}(t) \longrightarrow \mathbf{q}(t + \Delta t), \mathbf{v}(t + \Delta t) \\ \mathbf{q}(t), \mathbf{v}(t) \longrightarrow \mathbf{q}(t + \Delta t), \mathbf{v}(t + \Delta t) \\ \vdots \\ \mathbf{q}(t), \mathbf{v}(t) \longrightarrow \mathbf{q}(t + \Delta t), \mathbf{v}(t + \Delta t) \end{array} \right\} \\ \text{fit} \end{array} \right\} \rightarrow \psi(\bar{\mathbf{q}}, | \mathbf{x} + \mathbf{u}\Delta t, t + \Delta t). \tag{5}$$

The extra stress field  $\boldsymbol{\tau}$  can be determined in the course of these simulations by the virial theorem, or  $\nabla \cdot \boldsymbol{\tau}$  can be determined by summing the drag forces  $\gamma(\mathbf{v} - \mathbf{u})$  applied to the fluid.

In this brief outline, the PDF is important only as a mechanism to consolidate the internal degrees of freedom of the system. It implies also that the time scale over which polymer trajectories are computed,  $\Delta t$ , is equal to the time step of the continuum fluid solver. Used in this capacity, the dynamics of  $\psi$  are not important.

Mitran [22] proposed a modification of scheme (5) that allows the time steps to be decoupled, and, when  $\Delta t_{\text{polymer}} \ll \Delta t_{\text{fluid}}$ , can be made very efficient with time-domain parallelism. The idea is to find an *estimate* of  $\psi(t + \Delta t_{\text{fluid}})$  by solving some approximation to the applicable Fokker-Plank equation. With  $\psi(t)$  given, and estimate  $\psi(t + \Delta t_{\text{fluid}})$  determined, one can interpolate to approximate  $\psi(t_p = t + p\Delta t_{\text{polymer}})$  for any  $t \leq t_p \leq t + \Delta t_{\text{fluid}}$ . One then has a number of intervals of width  $\Delta t_{\text{polymer}}$ , each with an initial value, over which the SDE system (5) may be solved as an initial value problem. The final value of one interval should equal the initial value of the next, and this compatibility can be achieved though iteration. The strategy is a multiple

shooting method [4, 23], which can be implemented in parallel: the integrations over  $[t_p, t_{p+1}]$  can occur simultaneously. Upon convergence, estimates of  $\psi$  change – from values derived by Fokker-Plank approximation, to values consistent with the microscopic dynamics via (5).

The approximate Fokker-Plank method, or kinetic approximation, need not be strictly consistent with the underlying dynamics (3), but one is faced with a tradeoff between the accuracy of the kinetic approximation and time required to converge the multiple shooting method. The minimum accuracy requirement on the kinetic approximation is determined by the iteration scheme of the multiple shooting method. For example, if the approach is simple iteration then  $\psi_{\text{approx}}$  must be close enough to  $\psi_{\text{exact}}$  to ensure the overall scheme is a contractive mapping. If Newton-Raphson is employed then Kantorovich’s theorem [15] applies. In neither case does theory provide clear guidance. The approach we will take is to develop a method that is at least consistent with the Fokker-Plank equation, however even that may not be strictly necessary. For instance, Mitran [22] has shown that an approach based constructing  $\psi$  to minimize the the Kullback-Leibler distance [16] between an estimated macroscopic  $\boldsymbol{\tau}$  and the stress implied by  $\psi, \mathbf{u}$ , converges for a simple dumbbell model. In that case, estimation of  $\boldsymbol{\tau}$  by a constitutive approximation is used in place of a Fokker-Plank solution.

In the following section, a kinetic approximation based on the exact Fokker-Plank equation will be derived that is very simple to solve and faithful to the underlying equations, subject to the mean field assumption and overdamped ( $\gamma \rightarrow \infty$ ) conditions.

### 3 THE KINETIC APPROXIMATION

Associated with the constrained SDEs (3) is a Fokker-Plank equation for the probability density function (PDF)  $\psi(\mathbf{q}, t)$ , where  $\mathbf{q}$  represents the set of microscale configuration coordinates

$$\mathbf{q} = (\mathbf{q}_1 \ \mathbf{q}_2 \ \dots \ \mathbf{q}_N)^T \tag{6}$$

$$\mathbf{q}_i \in \mathbb{R}^D$$

$$\mathbf{q} \in \mathbb{R}^{ND}.$$

To obtain the Fokker-Plank equation associated with (3) we first rewrite the system without constraints. This can be accomplished by incorporating the constraints as Lagrange multipliers, with value given by an implicit function [11, 19]. The result can be written in block partitioned form

$$d\mathbf{p} = \mathbf{f}dt + \mathbf{g}d\mathbf{W} \tag{7}$$

$$\mathbf{p} = \begin{pmatrix} \mathbf{q} \\ \mathbf{v} \end{pmatrix} \tag{8}$$

$$\mathbf{f} = \begin{pmatrix} \mathbf{v} \\ \mathbf{F} \end{pmatrix} \tag{9}$$

$$\mathbf{g} = \begin{pmatrix} \mathbf{0} \\ \boldsymbol{\Gamma} \end{pmatrix} \tag{10}$$

where  $d\mathbf{W}$  is the set of independent Wiener derivatives,  $d\mathbf{W} = \boldsymbol{\xi}dt$  in  $\mathbb{R}^{ND}$ , analogous to (6). Forces exerted on the beads by the rods are given by

$$\mathbf{F}_i = \gamma(\mathbf{u}(\mathbf{q}_i) - \mathbf{v}_i) + \left[ (\Delta_{i-1}\mathbf{q})\mathbf{A}_{i-1,j}^{-1} - (\Delta_i\mathbf{q})\mathbf{A}_{i,j}^{-1} \right] \times [(\Delta_j\mathbf{q}) \cdot \gamma(\Delta_j\mathbf{u} - \Delta_j\mathbf{v}) + (\Delta_j\mathbf{v}) \cdot (\Delta_j\mathbf{v})] \tag{11}$$

and

$$\mathbf{\Gamma}_{ij} = \sigma \left\{ \mathbf{I} \delta_{ij} + \left[ (\Delta_{i-1} \mathbf{q}) \mathbf{A}_{i-1,j}^{-1} - (\Delta_i \mathbf{q}) \mathbf{A}_{i,j}^{-1} \right] (\Delta_j \mathbf{q})^T - \left[ (\Delta_{i-1} \mathbf{q}) \mathbf{A}_{i-1,j+1}^{-1} - (\Delta_i \mathbf{q}) \mathbf{A}_{i,j+1}^{-1} \right] (\Delta_{j+1} \mathbf{q})^T \right\}. \quad (12)$$

The  $i^{th}$  rod vector is denoted as  $\Delta_i \mathbf{q} = \mathbf{q}_{i+1} - \mathbf{q}_i$ , with  $\Delta_i \mathbf{q} = 0$ , if  $i < 1$  or  $i \geq N$ ,  $\mathbf{A}_{i,j}^{-1}$  denotes the  $(i, j)$  element of the  $\mathbf{A}^{-1}$  matrix, and  $\mathbf{A}$  is the  $(N-1) \times (N-1)$  tridiagonal matrix:

$$\mathbf{A}_{ij} = \begin{cases} -2(\Delta_i \mathbf{q}) \cdot (\Delta_i \mathbf{q}) & \text{if } i = j \\ (\Delta_i \mathbf{q}) \cdot (\Delta_j \mathbf{q}) & \text{if } |i - j| = 1 \\ 0 & \text{otherwise.} \end{cases} \quad (13)$$

Note that

$$\frac{1}{\sigma} \mathbf{\Gamma}_{ij} \mathbf{v}_j = \mathbf{v}_i + \left[ (\Delta_{i-1} \mathbf{q}) \mathbf{A}_{i-1,j}^{-1} - (\Delta_i \mathbf{q}) \mathbf{A}_{i,j}^{-1} \right] (\Delta_j \mathbf{q}) \cdot (\Delta_j \mathbf{v}); \quad (14)$$

$\mathbf{\Gamma}/\sigma$  projects a velocity field  $\mathbf{v}$  onto the space of velocities that obey the constraint

$$(\Delta_j \mathbf{q}) \cdot (\Delta_j \mathbf{v}) = 0, \quad (15)$$

which is the time derivative of (3c) [11]. The column space of  $\mathbf{\Gamma}$  is the space of velocities consistent with this constraint.

Note that we have included momentum in our SDEs, which implies the applicability of Itô calculus. It is not uncommon for momentum to be ignored (e.g., [19]) which then necessitates Stratonovich calculus (see also [17]). We will find that including momentum at this point leads to a simple form for the PDF because of the zero block in  $\mathbf{g}$  (10).

It follows from (7) and the rules of Itô differentiation that for any measurable function  $s(\mathbf{p})$  there exists the SDE

$$ds = \left[ \mathbf{f} \cdot \nabla_{\mathbf{p}} s + \frac{1}{2} (\mathbf{g} \mathbf{g}^T) : \nabla_{\mathbf{p}} \nabla_{\mathbf{p}} s \right] dt + (\mathbf{g} \cdot \nabla_{\mathbf{p}} s) d\mathbf{W}, \quad (16)$$

and so in expectation

$$d\langle s \rangle = \left\langle \mathbf{f} \cdot \nabla_{\mathbf{p}} s + \frac{1}{2} (\mathbf{g} \mathbf{g}^T) : \nabla_{\mathbf{p}} \nabla_{\mathbf{p}} s \right\rangle dt. \quad (17)$$

But, given the PDF, one also has

$$\langle s \rangle = \int d\mathbf{p} \Psi(\mathbf{p}, t) s(\mathbf{p}) \quad (18)$$

so

$$\begin{aligned} \frac{d\langle s \rangle}{dt} &= \int d\mathbf{p} \frac{\partial \Psi(\mathbf{p}, t)}{\partial t} s(\mathbf{p}) \\ &= \int d\mathbf{p} \Psi(\mathbf{p}) \left( \mathbf{f} \cdot \nabla_{\mathbf{p}} s + \frac{1}{2} (\mathbf{g} \mathbf{g}^T) : \nabla_{\mathbf{p}} \nabla_{\mathbf{p}} s \right). \end{aligned} \quad (19)$$

Note that here we have introduced  $\Psi(\mathbf{q}, \mathbf{v}, t)$ , a function of all dynamic variables, which is different from the PDF  $\psi(\mathbf{q}, t)$  we desire for our kinetic approximation. We integrate this expression with respect to time, then twice by parts with  $\Psi$  and  $\nabla\Psi$  zero at infinity. The result is

$$0 = \int dt \int d\mathbf{p} s \left( \frac{\partial\Psi}{\partial t} + \nabla_{\mathbf{p}} \cdot (\mathbf{f}\Psi) - \nabla_{\mathbf{p}(i)} \nabla_{\mathbf{p}(j)} \left( \frac{1}{2}(\mathbf{g}\mathbf{g}^T)_{ij}\Psi \right) \right), \quad (20)$$

giving the Fokker-Planck equation

$$\frac{\partial\Psi}{\partial t} + \nabla_{\mathbf{p}} \cdot (\mathbf{f}\Psi) - \nabla_{\mathbf{p}(i)} \nabla_{\mathbf{p}(j)} \left( \frac{1}{2}(\mathbf{g}\mathbf{g}^T)_{ij}\Psi \right) = 0 \quad (21)$$

in the space of coordinates and particle velocity, and containing both drift and diffusion contributions. Substituting the block partitions of  $\mathbf{f}$  (9) and  $\mathbf{g}$  (10), it is apparent that the diffusion term is only associated with the velocity coordinates:

$$\frac{\partial\Psi}{\partial t} = -\mathbf{v} \cdot \nabla_{\mathbf{q}}\Psi - \nabla_{\mathbf{v}} \cdot (\mathbf{F}\Psi) + \frac{1}{2}\mathbf{\Gamma}_{ik}\mathbf{\Gamma}_{jk} \frac{\partial^2\Psi}{\partial\mathbf{v}_i\partial\mathbf{v}_j} \quad (22)$$

where  $\mathbf{\Gamma}$  depends on  $\mathbf{q}$  but not  $\mathbf{v}$ .

At this point we note that the momentum coordinates evolve rapidly relative to the position coordinates because of the magnitude of  $\gamma$ . We use adiabatic elimination to remove these fast modes from the Fokker-Planck equation [25]. Assuming the decomposition  $\Psi(\mathbf{q}, \mathbf{v}, t) = \psi(\mathbf{q}, t)\varphi(\mathbf{v})$ , for  $\varphi$  to be stationary one has

$$\frac{\partial}{\partial\mathbf{v}_i} \cdot \left[ -\mathbf{F}_i + \frac{1}{2}\mathbf{\Gamma}_{ik}\mathbf{\Gamma}_{jk} \frac{\partial}{\partial\mathbf{v}_j} \right] \varphi = 0. \quad (23)$$

We assume that this holds for each  $i$ , and that the  $D$  components of  $\mathbf{v}_i$  are also independent. These assumptions are motivated by the fact that velocity is very nearly  $\delta$ -correlated along a polymer chain [7, 11]. With these assumptions,

$$-\mathbf{F}_i\varphi + \frac{1}{2}\mathbf{\Gamma}_{ik}\mathbf{\Gamma}_{jk} \frac{\partial}{\partial\mathbf{v}_j} \varphi = \mathbf{c}_i \quad (24)$$

for some vector  $\mathbf{c}_i$  that is independent of  $\mathbf{v}_i$ . Now integrate (24) with respect to velocity over the entire velocity space  $[-\infty, +\infty]^{DN}$ :

$$\int d\mathbf{v}\mathbf{c}_i = -\langle\mathbf{F}_i\rangle + \frac{1}{2}\mathbf{\Gamma}_{ik}\mathbf{\Gamma}_{jk} \int d\mathbf{v}\nabla_{\mathbf{v}_j}\varphi. \quad (25)$$

The integral on the right hand side must be zero since  $\varphi$  and its gradient must be zero at infinity. Then, if expectation  $\langle\mathbf{F}_i\rangle$  is bounded, it follows that the integral on the left hand side must be bounded:  $\mathbf{c}_i = 0$  and therefore  $\langle\mathbf{F}_i\rangle = 0$ .

This convenient result is not unexpected.  $\mathbf{F}_i$  is the smooth part of the acceleration experienced by bead  $i$ ,  $\gamma(\mathbf{u}_i - \mathbf{v}_i)$ , projected onto the space of accelerations that satisfy the second derivative of the holonomic constraint (3c).  $\langle\mathbf{F}_i\rangle$  being zero signifies that subject to constraints,  $\langle\mathbf{v}_i\rangle = \mathbf{u}_i$ , which is the behavior anticipated in the limit  $\gamma \rightarrow \infty$  that motivates adiabatic elimination in the first place.

$\mathbf{\Gamma}$  has dimension  $(ND) \times (ND)$ , but is a surjective (many-to-one) mapping so  $\mathbf{\Gamma}^{-1}$  is not defined. Its column space is the space of velocities compatible with the velocity constraint.  $\mathbf{F}$  is a  $(ND) \times 1$  dimensional vector in the space of accelerations compatible with the acceleration

constraint. These spaces are not identical, in general, but they are equated in (24) as a consequence of applying (23) separately to each degree of freedom. Let us formally restrict (23) (with  $\mathbf{c}_i = 0$ ) to the column space of  $\mathbf{\Gamma}$ ,

$$-\mathbf{\Gamma}_{\ell i} \mathbf{F}_i \varphi + \frac{1}{2} \mathbf{\Gamma}_{\ell i} \mathbf{\Gamma}_{ik} \mathbf{\Gamma}_{jk} \frac{\partial}{\partial \mathbf{v}_j} \varphi = 0 \quad (26)$$

then use the idempotence property of projection  $\mathbf{\Gamma}/\sigma$  to obtain

$$-\mathbf{\Gamma}_{\ell i} \mathbf{F}_i \varphi + \frac{\sigma}{2} \mathbf{\Gamma}_{\ell k} \mathbf{\Gamma}_{jk} \frac{\partial}{\partial \mathbf{v}_j} \varphi = 0. \quad (27)$$

Although  $\mathbf{\Gamma}\mathbf{\Gamma}^T$  does not possess an inverse, we can use the Moore-Penrose pseudoinverse ( $\dagger$ ) to write

$$-\frac{2}{\sigma} (\mathbf{\Gamma}\mathbf{\Gamma}^T)_{j\ell}^\dagger \mathbf{\Gamma}_{\ell i} \mathbf{F}_i \varphi + \frac{\partial}{\partial \mathbf{v}_j} \varphi = 0. \quad (28)$$

This is equivalent to the normal equations; a least squares mapping of accelerations  $\mathbf{F}\varphi$  to  $\varphi_{\mathbf{v}}$ . Integration of (28) gives

$$\varphi \propto \exp \left( \frac{2}{\sigma} \int d\mathbf{v}'_j{}^T [\mathbf{\Gamma}\mathbf{\Gamma}]_{j\ell}^\dagger \mathbf{\Gamma}_{\ell i} \mathbf{F}_i \right). \quad (29)$$

Upon integrating (22) with respect to  $\mathbf{v}$  to eliminate the fast modes, the Fokker-Planck dynamics (23) reduce to

$$\frac{\partial \psi}{\partial t} = \bar{\mathbf{v}} \cdot \nabla_{\mathbf{q}} \psi \quad (30a)$$

with

$$\bar{\mathbf{v}}(\mathbf{q}) = \int^* d\mathbf{v} \mathbf{v} \varphi \quad (30b)$$

$$= \frac{\int^* d\mathbf{v} \mathbf{v} \exp \left( \frac{2}{\sigma} \int d\mathbf{v}'_j{}^T [\mathbf{\Gamma}\mathbf{\Gamma}]_{j\ell}^\dagger \mathbf{\Gamma}_{\ell i} \mathbf{F}_i \right)}{\int^* d\mathbf{v} \exp \left( \frac{2}{\sigma} \int d\mathbf{v}'_j{}^T [\mathbf{\Gamma}\mathbf{\Gamma}]_{j\ell}^\dagger \mathbf{\Gamma}_{\ell i} \mathbf{F}_i \right)} \quad (30c)$$

being the vector of average velocities. The asterisk signifies that the integral is over the space of velocities consistent with the derivative constraint (15). A more formal derivation would use internal coordinates, but we find that obscures the essential result.

When  $\bar{\mathbf{v}}$  does not vary with  $\mathbf{q}$ , result (30) has a trivial solution,

$$\psi(\mathbf{q}, t + \Delta t) = \psi(\mathbf{q} - \bar{\mathbf{v}}\Delta t, t) : \quad (31)$$

the PDF is advected (in  $\mathbb{R}^{ND}$ ) with velocity  $\bar{\mathbf{v}}$ . In the general case of variable  $\bar{\mathbf{v}}(\mathbf{q})$ ,  $\psi$  given by (31) is consistent with (30). That is,  $\psi$  (31) obeys a modified equation [27] that reduces to (30) in the limit  $\Delta t \rightarrow 0$  (see also [8, 9, 20] for the homogenized transport approach). We will analyze  $\bar{\mathbf{v}}$  further below, and show that it is related to  $\mathbf{u}$ , the fluid velocity at the polymer center of mass. The analysis indicates that  $\bar{\mathbf{v}}$  does not vary significantly with  $\mathbf{q}$  when making a physically reasonable hypothesis, justifying (31), and giving rise to a practical algorithm for its solution.

It can be shown that  $\bar{\mathbf{v}}$  is approximately normally distributed with variance  $k_B T/m$  and mean

$$\mathbf{u}' = \frac{1}{\sigma} \mathbf{\Gamma} \mathbf{u}, \quad (32)$$

the projection of  $\mathbf{u}$  onto the velocity constraint manifold.

For given  $\mathbf{u}$ , every velocity  $\mathbf{v}'$  maps to some velocity  $\mathbf{v}''$  through the projections  $\mathbf{F}$  and  $\mathbf{\Gamma}$ :

$$\gamma(\mathbf{u}' - \mathbf{v}'') = \frac{1}{\sigma} \mathbf{\Gamma} \mathbf{F} \quad (33)$$

where  $\mathbf{v}'' = (\mathbf{\Gamma}/\sigma)\mathbf{v}''$ :  $\mathbf{v}''$  is on the velocity constraint manifold. Using that mapping,

$$\psi \propto \exp \left( 2\gamma \int \varrho(\mathbf{v}'') d\mathbf{v}''^T_j [\mathbf{\Gamma} \mathbf{\Gamma}]_{ji}^\dagger (\mathbf{u}' - \mathbf{v}'')_i \right) \quad (34)$$

where  $\varrho(\mathbf{v}'')$  is the Jacobian determinant, the density of the  $\mathbf{v}' \mapsto \mathbf{v}''$  mapping.

A simple algorithm, and one for which numerical simulations show qualitatively correct viscoelastic effect capture, is obtained by positing  $\varrho = \text{constant}$ . Then,

$$\psi \propto \exp \left( 2\gamma \int d\mathbf{v}''^T_j [\mathbf{\Gamma} \mathbf{\Gamma}]_{ji}^\dagger (\mathbf{u}' - \mathbf{v}'')_i \right) \quad (35a)$$

$$\propto \exp \left( -2\gamma (\mathbf{u}' - \mathbf{v}'')^T_j [\mathbf{\Gamma} \mathbf{\Gamma}]_{ji}^\dagger (\mathbf{u}' - \mathbf{v}'')_i \right) \quad (35b)$$

$$\psi(\mathbf{q}, \mathbf{v}'') \propto \exp \left( -\frac{m}{k_B T} (\mathbf{u}' - \mathbf{v}'')^2 \right). \quad (35c)$$

In the last step, we use  $\sigma(\mathbf{u}' - \mathbf{v}'') = \mathbf{\Gamma}(\mathbf{u}' - \mathbf{v}'')$  and substitute (4). With this approximation, (30c) becomes

$$\bar{\mathbf{v}} = \frac{\int^* d\mathbf{v} \mathbf{v} \left( -\frac{m}{k_B T} (\mathbf{u}' - \mathbf{v})^2 \right)}{\int^* d\mathbf{v} \left( -\frac{m}{k_B T} (\mathbf{u}' - \mathbf{v})^2 \right)} = \mathbf{u}'. \quad (36)$$

The result (36) indicates that  $\bar{\mathbf{v}}$  is indeed approximately constant if the  $\mathbf{v}' \mapsto \mathbf{v}''$  mapping is volume preserving. This corresponds to assuming that the distribution of polymer bead velocities is strongly peaked around configurations that satisfy the rigid-rod constraints.

For the solution of (31), we propose the following two stage process. First, separate internal coordinates into a mean part  $\mathbf{x}$  and a deviation  $\bar{\mathbf{q}}$ ,

$$\bar{\mathbf{q}}_i = \mathbf{q}_i - \mathbf{x} \quad (37)$$

and represent the PDF in form  $\psi(\bar{\mathbf{q}} | \mathbf{x}, t)$ . Then, draw a random velocity vector  $\mathbf{v} \in \mathbb{R}^{ND}$  with mean 0 and variance  $k_B T/m$ , and project it onto the constraint manifold

$$\mathbf{v} := \frac{1}{\sigma} \mathbf{\Gamma} \mathbf{v}. \quad (38)$$

Let  $\bar{\mathbf{v}}$  be the mean of the  $N$  partitions  $\mathbf{v}_i$ , and define

$$\delta\mathbf{v} = \mathbf{v} - \begin{pmatrix} \bar{\mathbf{v}} \\ \bar{\mathbf{v}} \\ \vdots \\ \bar{\mathbf{v}} \end{pmatrix}. \quad (39)$$

Then,

$$\psi_{\text{adv}}(\bar{\mathbf{q}} \mid \mathbf{x} - [\bar{\mathbf{v}} + \mathbf{u}(\mathbf{x})]\Delta t, t) \quad (40)$$

is the PDF in relative coordinates  $\bar{\mathbf{q}}$  about center  $\mathbf{x}$  at time  $t + \Delta t$ . Here  $\mathbf{x}$  and  $\mathbf{u}(\mathbf{x})$  are in  $\mathbb{R}^D$  – this is Lagrangian advection in physical coordinates.

One possible interpretation of (40) is that the discretization of  $\psi(\bar{q})$  be Lagrangian, and that it be transported with velocity  $\bar{\mathbf{v}} + \mathbf{u}$ . Another interpretation is that  $\psi(\bar{q})$  be discretized on a spatial (Eulerian) grid. In that case, let  $\mathbb{S}$  be a set of discretization points  $\mathbf{x}_j$  such that

$$\mathbf{x} - [\bar{\mathbf{v}} + \mathbf{u}(\mathbf{x})]\Delta t = \sum_{j \in \mathbb{S}} w_j \mathbf{x}_j \quad (41a)$$

$$\sum w_j = 1 \quad (41b)$$

$$w_j \geq 0 \quad \forall j. \quad (41c)$$

Then,

$$\psi_{\text{adv}}(\bar{\mathbf{q}} \mid \mathbf{x} - [\bar{\mathbf{v}} + \mathbf{u}(\mathbf{x})]\Delta t, t) = \sum_{j \in \mathbb{S}} w_j \psi(\bar{\mathbf{q}} \mid \mathbf{x}_j, t). \quad (42)$$

This first step accounts for the mean velocity. The change about the mean comes from evaluating (40) at relative coordinate  $\hat{\mathbf{q}}$

$$\hat{\mathbf{q}} = \mathbb{P}_{\mathbf{q}} \left[ \bar{\mathbf{q}} - \Delta t \delta\mathbf{v} - \Delta t \begin{pmatrix} \bar{\mathbf{q}}_1 \cdot \nabla \mathbf{u}(\mathbf{x}) \\ \bar{\mathbf{q}}_2 \cdot \nabla \mathbf{u}(\mathbf{x}) \\ \vdots \\ \bar{\mathbf{q}}_N \cdot \nabla \mathbf{u}(\mathbf{x}) \end{pmatrix} \right]. \quad (43)$$

Here  $\mathbb{P}_{\mathbf{q}}$  is the projection onto (3c) (e.g., [6]).

Altogether, for absolute coordinate  $\mathbf{q}$ ,

$$\psi_{\text{adv}}(\hat{\mathbf{q}}(\mathbf{q}, \mathbf{x}, \mathbf{v}, \Delta t \nabla \mathbf{u}) \mid \mathbf{x} - [\bar{\mathbf{v}} + \mathbf{u}(\mathbf{x})]\Delta t, t) \quad (44)$$

provides one sample of  $\psi(\bar{\mathbf{q}} \mid \mathbf{x}, t + \Delta t)$ . The sample is subject to statistical error because of the random velocity  $\mathbf{v}$  which accounts for the diffusive part of the Fokker-Plank equation.

We note that this statistical error is amenable to the variance reduction approach of Chorin [5]. In fact, the use of a random vector  $\mathbf{v}$  is not necessary because of result (36). Its inclusion provides our kinetic approximation with the diffusive character exhibited by the Fokker-Plank equation (21). The diffusivity there is large because

$$\mathbf{\Gamma} \mathbf{\Gamma}^T \frac{\partial^2 \psi}{\partial \mathbf{v}^2} = \mathcal{O}(1) \psi. \quad (45)$$

Another source of diffusion is the numerical diffusion associated with interpolation (41). With  $h$  as the spatial discretization length, the numerical diffusion term is approximately

$$\frac{h^2}{\Delta t} |\nabla^2 \psi|, \quad (46)$$

which is negligible by comparison to (45) for typical parameters.

This algorithm is first-order accurate in time. Higher order can be attained using a variety of high-order ODE approaches, depending on the relative time centering of  $\mathbf{u}$  and  $\psi$ .

#### 4 Numerical Results

To demonstrate an application of the approach we simulate the flow of a viscoelastic fluid in a 4:1 contraction (2D). We discretize  $\psi$  with Lagrangian markers, which have a mean density of 10 per cell. These are initially placed randomly, and the PDFs initially describe a fully relaxed polymer (all angles are equally probable). The PDF representation models the angle of each Kramers “rod” with respect to fixed coordinate axes of the simulation. The distribution of this single angle is modeled simply through the radii of gyration. Those markers swept out of the domain in a given time step are replaced on the left inflow boundary so the number is fixed. On inflow, the marker PDFs are fully relaxed. The numerical method used to solve the continuum equations is the stationary-geometry specialization of the method presented in [21]. Each PDF is sampled 400 times per time step of the method, and  $\nabla \cdot \boldsymbol{\tau}$  is averaged over drag forces with variance reduction after [26]. Figure 1 displays the vector field  $\nabla \cdot \boldsymbol{\tau}$  in a  $256 \times 192$  cell simulation of an  $\text{Re} \approx 1$  flow computed with a time step corresponding with a Courant-Friedrichs-Lewy number of 0.75. Physical parameters approximate a 10 Kuhn-length segment of  $\lambda$ -phage DNA in water:  $\rho = 1 \text{ g/cm}^3$ ,  $m = 10^{-19} \text{ g}$ ,  $a = 7 \times 10^{-6} \text{ m}$ ,  $\gamma = 10^{12} \text{ s}^{-1}$ ,  $\sigma = 5.1 \times 10^6 \text{ m/s}^{3/2}$ . This stress divergence term is a source term to the continuum scale solver. The calculated  $\nabla \cdot \boldsymbol{\tau}$  is amplified by a factor of  $10^3$  (i.e., each simulated polymer is assumed to represent a population of  $10^3$  polymers).

While the computational work is substantial, the use of the intermediate kinetic scale results in great simplification relative to the CONNFESSIT model. From time level to time level we stored a 2-parameter PDF for  $3 \times 10^5$  Lagrangian markers, each of which generated 400 representative polymers in a time step. In the equivalent CONNFESSIT approach  $1.2 \times 10^8$  polymers would be tracked from time step to time step, each having 20 coordinate degrees of freedom. The next step in our program is to use this approximation to the Fokker-Planck equation as a predictor in the time-parallel framework of Mitran [22].

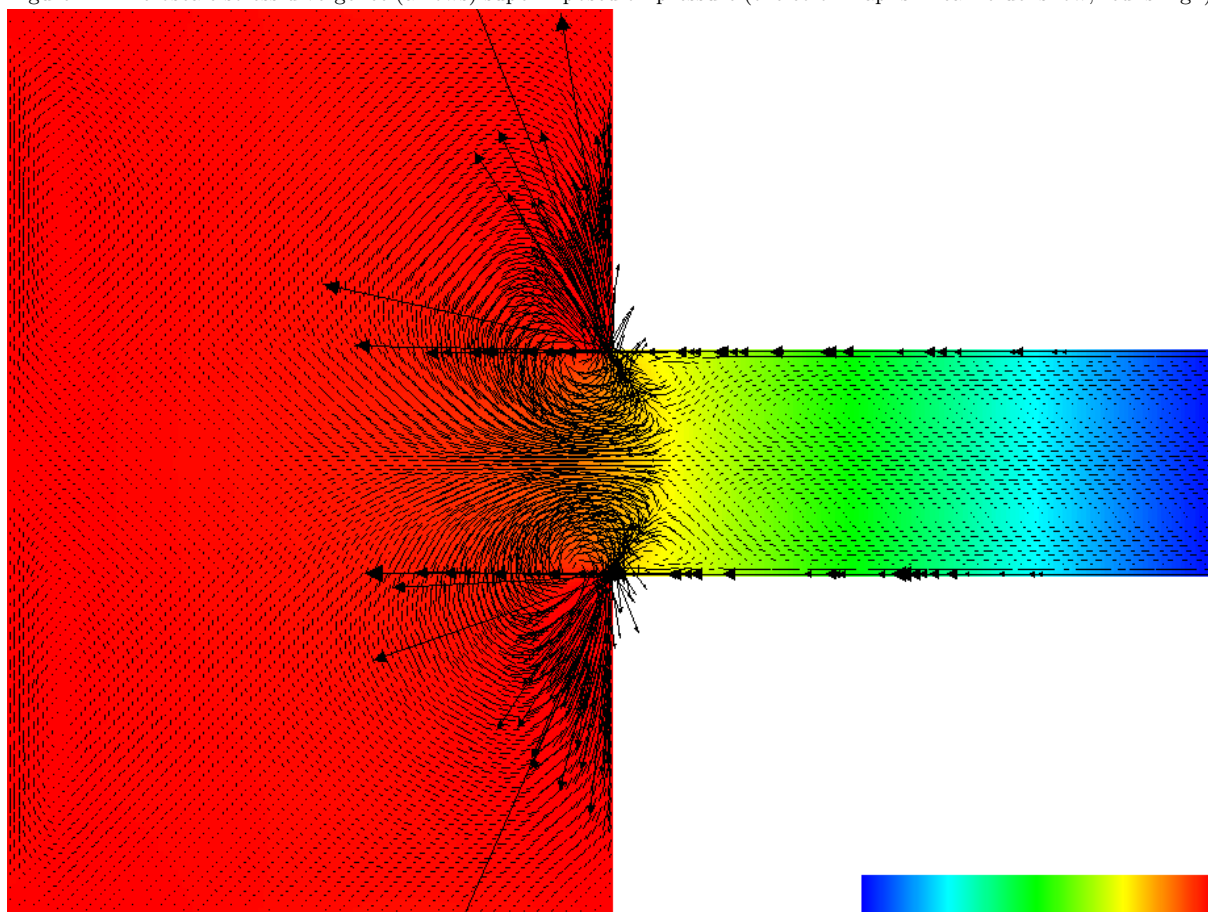
#### ACKNOWLEDGEMENTS

G.H. Miller, S. Mitran, and D. Trebotich were supported by the U.S. Department of Energy Office of Advanced Scientific Computing Research under grants DE-SC0001981 and A10-0486-001, and contract DE-AC02-05-CH11231, respectively.

#### References

- [1] A. N. Beris and B. J. Edwards. *Thermodynamics of flowing systems with internal microstructure*. Oxford, 1994.
- [2] B. R. Bird, C. F. Curtiss, R. C. Armstrong, and O. Hassager. *Dynamics of Polymeric Liquids, Kinetic Theory*. Wiley-Interscience, 1987.
- [3] R. B. Bird, P. J. Dotson, and N. L. Johnson. Polymer solution rheology based on a finitely extensible bead-spring chain model. *J. Non-Newtonian Fluid Mech.*, 7:213–235, 1980.
- [4] R. Bulirsch. Die Mehrzielmethode zur numerischen Lösung von nichtlinearen Randwertproblemen und Aufgaben der optimalen Steuerung. Report of the Carl-Cranz-Gesellschaft, Oberpfaffenhofen, Germany, 1971.

Figure 1. Microscale stress divergence (arrows) superimposed on pressure (the color map is linear: blue is low, red is high).



- [5] A. J. Chorin. Hermite expansions in Monte-Carlo computation. *J. Comput. Phys.*, 8:472–482, 1971.
- [6] G. Ciccotti, M. Ferrario, and J.-P. Ryckaert. Molecular dynamics of rigid systems in Cartesian coordinates. A general formulation. *Molec. Phys.*, 47:1253–1264, 1982.
- [7] S.F. Edwards and A.G. Goodyear. The velocity distribution function for a polymer chain. *J. Phys. A Gen. Phys.*, 5:1188–1195, 1972.
- [8] R. Grimshaw, D. Pelinovsky, and E. Pelinovsky. Homogenization of the variable-speed wave equation. *Wave Motion*, 47:496–507, 2010.
- [9] T. Hou and X. Xin. Homogenization of linear transport equations with oscillatory vector fields. *SIAM J. Appl. Math.*, 52:34–45, 1992.
- [10] B. Kallemov. *A higher-order multiscale method for polymer-laden flows*. PhD thesis, Dept. Applied Science, Univ. California, Davis, 2011.
- [11] B. Kallemov and G.H. Miller. A second-order strong method for the Langevin equations with holonomic constraints. *SIAM J. Sci. Comput.*, 33:653–676, 2011.
- [12] B. Kallemov, G.H. Miller, and D. Trebotich. A Duhamel approach for the Langevin equations with holonomic constraints. *Mol. Simulat.*, 35:440–447, 2009.
- [13] B. Kallemov, G.H. Miller, and D. Trebotich. Numerical simulation of polymer flow in microfluidic devices. In *Proc. Fourth SIAM Conference on Mathematics for Industry*, pages 93–98, 2010.
- [14] B. Kallemov, G.H. Miller, and D. Trebotich. A higher-order accurate fluid-particle algorithm for polymer flows. *Mol. Simulat.*, 37:738–745, 2011.
- [15] L. V. Kantorovich. Functional analysis and applied mathematics. *Usp. Mat. Nauk*, 3(6):89–185, 1948. in Russian. Translated by C. D. Benster as National Bureau of Standards report 1509, 1952.
- [16] S. Kullback and R. A. Leibler. On information and sufficiency. *Ann. Math. Stat.*, 22:79–86, 1951.
- [17] R. Kupferman, G.A. Pavliotis, and A.M. Stuart. Itô versus Stratonovich white-noise limits for systems with inertia and colored multiplicative noise. *Phys. Rev. E*, 70(036120), 2004.
- [18] M. Laso and H.C. Öttinger. Calculation of viscoelastic flow using molecular models: the CONNFESSIT approach. *J. Comput. Phys.*, 47:1–20, 1993.
- [19] T.W. Liu. Flexible polymer chain dynamics and rheological properties in steady flows. *J. Chem. Phys.*, 90:5826–5842, 1989.
- [20] D. McLaughlin, G.C. Papanicolaou, and O.R. Pironneau. Convection of microstructure and related problems. *SIAM J. Appl. Math.*, 45:780–797, 1985.
- [21] G. H. Miller and D. Trebotich. An embedded boundary method for the Navier-Stokes equations on a time-dependent domain. *Comm. App. Math. Comp. Sci.*, 2011. in press.
- [22] S. Mitran. Time parallel kinetic-molecular interaction algorithm for CPU/GPU computers. *Proc. Comp. Sci.*, 1:745–752, 2010.

- [23] D. D. Morrison, J. D. Riley, and J. F. Zangarano. Multiple shooting method for two-point boundary value problems. *Comm. ACM*, 5(12):613–614, 1962.
- [24] J. G. Oldroyd. On the formulation of rheological equations of state. *Proc. Roy. Soc. London A*, 200:523–541, 1950.
- [25] H. Risken. *The Fokker Planck Equation*. Springer-Verlag, 2nd edition, 1989.
- [26] N.J. Wanger and H.C. Öttinger. Accurate simulation of linear viscoelastic properties by variance reduction through the use of control variates. *J. Rheol.*, 41:757–768, 1997.
- [27] R. F. Warming and B. J. Hyett. The modified equation approach to the stability and accuracy analysis of finite-difference methods. *J. Comput. Phys.*, 14:159–179, 1974.